RARAF – Table of Contents

RARAF PROFESSIONAL STAFF

RARAF Staff *(l–r)*: Guy Garty, Yanping Xu, Andrew Harken, David Brenner, Sasha Lyulko, Gerhard Randers-Pehrson, Stephen Marino, Alan Bigelow, Brian Ponnaiya and Charles Geard. *Not shown*: Giuseppe Schettino, Gregory Ross and Gloria Jenkins-Baker.

David J. Brenner, Ph.D., D.Sc. **–** RARAF Director
Stephen A. Marino, M.S. **–** RARAF Manager
Gerhard Randers-Pehrson, Ph.D. **–** RARAF Associate Director, Chief Physicist
Charles R. Geard, Ph.D. – CRR Associate Director, Senior Biologist
Alan Bigelow, Ph.D. – Associate Research Scientist
Brian Ponnaiya, Ph.D. – Associate Research Scientist
Guy Y. Garty, Ph.D. – Staff Associate
Gregory Ross, M.S. – Programmer Analyst
Giuseppe Schettino, Ph.D. – Post-Doctoral Research Scientist
Yanping Xu, Ph.D. – Post-Doctoral Research Scientist
Andrew Harken, Ph.D. – Post-Doctoral Research Scientist
Gloria Jenkins-Baker, B.A. – Biology Technician

The Radiological Research Accelerator Facility

AN NIH-SUPPORTED RESOURCE CENTER – WWW.RARAF.ORG

Director: David J. Brenner, Ph.D., D.Sc.
Associate Director: Gerhard Randers-Pehrson, Ph.D.
Manager: Stephen A. Marino, M.S.

Introduction

This has been another momentous year for RARAF:

- RARAF is now 40 years old. It was started January 1, 1967 with the transfer of the 4.2 MV Van de Graaff that had been the injector for the Cosmotron at Brookhaven National Laboratory.
- Construction of over 2000 square feet of laboratory and office space was completed on the third floor, and was funded by a contribution from Columbia University.
- The new Singletron accelerator completed its first year of use.

Research using RARAF

The "bystander" effect, in which cells that are not irradiated show a response to radiation when in close contact with or even only in the presence of irradiated cells, continues to be the main focus of the biological experiments at RARAF, especially those using the microbeam. All but one of the biology experiments run this year examined this effect, observing a variety of endpoints to determine the size of the effect and the mechanism(s) by which it is transmitted. Evidence continues to be obtained for both direct gap junction communication through cell membrane contact and indirect, long-range communication through the cell media. Both the microbeam and the track segment facilities continue to be utilized in various investigations of this phenomenon. The single-particle Microbeam Facility provides precise control of the number and location of particles so that irradiated and bystander cells may be distinguished, but is somewhat limited in the number of cells that can be irradiated. The Track Segment Facility provides broad beam irradiation that has a random pattern of charged particles but allows large numbers of cells to be irradiated and multiple users in a single day.

Two special types of track segment dishes are being used to investigate the bystander effect using the Track Segment Facility: double-sided dishes and "strip" dishes. Double-sided dishes have Mylar foils glued on both sides of a stainless steel ring, 1cm apart, with cells plated on the inside surfaces of both foils. The interior is completely filled with medium. This type of dish is used for investigation of the non-contact, long-range bystander effect since the cells on the two surfaces are not in direct contact, can only communicate through the culture medium, and only the cells on one surface are irradiated. "Strip" dishes consist of a stainless steel ring with Mylar foil glued to one side in which a second dish is inserted. The Mylar foil glued to the inner dish has alternate strips of the Mylar removed. Cells are plated over the combined surface and are in contact. The Mylar on the inner dish is thick enough to stop the charged particles (usually ^{4}He ions) and the cells plated on it are not irradiated. These dishes are used for bystander experiments involving cell-to-cell communication.

Interest in irradiation of 3D systems has increased this past year, with several experimenters irradiating tissue samples using either helium ions or protons. Imaging systems for the Microbeam Facility are being developed to enable observation and targeting of cells that are not in monolayers; in the interim, cultured human tissue samples are being irradiated using the Track Segment Facility. The tissue samples are on membranes on the end of cylindrical plastic holders. Plastic discs have been constructed that fit in the spaces in the irradiation wheel and have small holes to provide precise alignment of the feet that are around the bottom edges of the tissue holders. A hole in the middle of each disc is fitted with two stainless steel half-discs that have a precise 0.001" (25μm) space between them. The tissue membrane is in contact with the stainless steel, which is thick enough to stop the charged particles. This provides a narrow line of irradiation across the center of the entire sample. The tissue samples are later sectioned, either parallel or crosswise to the line of irradiation, to observe bystander effects as a function of distance from the line of irradiation.

Table 1 lists the experiments performed at RARAF from January 1 through December 31, 2006 and the number of days each was run in this period. Use of the accelerator for experiments was over 59% of the normal available time, 6% higher than last year, which had been the highest we had attained at Nevis Labs. Fourteen different experiments were run during this period, about the average for 2000-2005. Eight experiments were undertaken by members of the CRR, supported by grants from the National Institutes of Health (NIH), the National Aeronautics and Space Administration (NASA), and the Department of Energy (DOE). Six experiments were performed by outside users, supported by grants and awards from NASA, the NIH, the DOE, the Japanese Nuclear Energy Crossover Research Program and the Japanese 21st Century Center of Excellence Program. Brief descriptions of these experiments follow.

Gerhard Randers-Pehrson and Alan Bigelow of the CRR continued development of a method to detect explosives in baggage (Exp. 82). The detection system is based on resonant elastic scattering of 0.43MeV neutrons by nitrogen and oxygen. Measurements of the neutron transmission through a liquid nitrogen sample were made using neutrons produced in a very thin target by the 7Li(p,n) reaction. A high voltage is applied to the target and scanned slowly up and down

Table 1. Experiments Run at RARAF, January 1 – December 31, 2006

Exp. No.	Experimenter	Institution	Exp. Type	Experiment Title	No. Days Run
82	G. Randers-Pehrson A. Bigelow	CRR	Physics	Detection of explosives	27.8
89	R.H. Maurer D. Roth J. Goldsten	Johns Hopkins University	Physics	Calibration of a portable real-time neutron spectrometry system	2.3
103	B. Hu C.R. Geard	CRR	Biology	Damage induction and characterization in known hit versus non-hit human cells	25.3
106	B. Ponnaiya C.R. Geard	CRR	Biology	Track segment α-particles, cell co-cultures and the bystander effect	6.2
110	H Zhou Y-C. Lien T.K. Hei	CRR	Biology	Identification of molecular signals of α-particle-induced by-stander mutagenesis	38.2
126	O. Sedelnikova W. Bonner (G. Jenkins)	NIH	Biology	γ-H2AX foci formation in directly irradiated and bystander cells	3.5
130	B. Ponnaiya C.R. Geard	CRR	Biology	Investigation of bystander responses in 3-dimensional systems	8.5
132	T. Funayama	JAEA	Biology	Quantitative analysis of the relationship between bystander response and DNA double strand breaks	9.8
133	J. Ahn, S. Ghandhi S. Amundson	CRR	Biology	Bystander effects in primary cells	9.4
134	P. Grabham C.R. Geard	CRR	Biology	Effects of track segment low-energy particles versus high-energy space-related radiations	1.3
135	K. Suzuki M. Yamauchi	Nagasaki University	Biology	Visualization of the effects of radiation on chromatin structure in bystander cells using 53BP1 foci as markers of chromatin disorganization	3.0
136	S. Amundson G. Schettino S. Paul	CRR	Biology	Bystander effects in 3D tissues	3.8
137	S. Bailey S.E. Williams (B. Ponnaiya)	Colorado State University	Biology	TRF2 recruitment in cells irradiated with α-particles	6.5
138	E. Azzam J. Santos O. Kovalenko	NJSMD	Biology	Investigation of the effect of mtDNA damage on apoptosis in hTERT cells	2.3

Note: Names in parentheses are members of the CRR who collaborated with outside experimenters.

across the proton energy required to produce neutrons with the required energy. The neutron transmission can then be measured over the range of a few keV under identical target and focusing conditions.

Richard Maurer, David Roth and John Goldsten of Johns Hopkins University continued the characterization of a neutron spectrometry system (Exp. 89) that may be used on the International Space Station and possibly the manned mission to Mars. They evaluated a tin-walled helium-3 gas detector with 0.84MeV neutrons for energy calibration and response. This detector is similar to a detector delivered to NASA Marshall Space Flight Center for a future balloon flight. The acquisition and pre-trigger times were the same as the balloon flight instrument and the detector was sampled at a data rate that accurately defined the acquired waveforms. A newly fabricated Eljen boron-loaded scintillator was evaluated for both energy calibration and waveform distributions at six neutron energies from 0.84 to 14MeV. This energy range is of primary concern when determining the neutron energy spectra produced in high energy collisions of protons and heavy ions with thick spacecraft material targets. Several acquisition parameters were altered to determine their effect on the recoil peak, capture peak and energy resolution. A recently refurbished 5mm thick silicon detector that is almost 5 times the diameter of the previously used silicon detectors was evaluated with 14MeV neutrons. Due to the increased area and consequent increased oblique path lengths, the response function used for the smaller 5mm detector needed to be modified.

Charles Geard and Burong Hu of the CRR continued

studies of the bystander effect, examining the relationship between the radiation-induced bystander response and genomic instability (Exp. 103). Normal human fibroblasts were cultured in double-sided Mylar dishes (see above) and one side was irradiated with 3Gy of ^{4}He ions using the Track Segment Facility. The range of the helium ions is very much shorter than the space between the two Mylar layers so that the cells on the other side of the dish were then bystanders, which could only be influenced by signal transfer through the medium. For microbeam studies, 20% of the nuclei of nearly confluent (in contact) fibroblasts were irradiated with 30 ^{4}He ions each, which ensures that only non-hit bystander cells can survive over many cell generations. In both scenarios cells were harvested at specific time points post-irradiation. Elevated levels of chromosomal damage in bystander cells were observed after G_2 PCC, reflecting signal transfer from irradiated cells and suggesting there is genomic instability in bystander cells after track segment and microbeam irradiation of cells. Preliminary mFISH results 5 cell divisions post-irradiation show chromosome 1 and 3 more frequently damaged in both of the experimental protocols. Experiments are continuing in order to confirm this interesting finding and investigate the signal transfer in bystander effect and genomic instability between the two kinds of irradiations.

Two other studies investigating the bystander effect were continued by Brian Ponnaiya and Charles Geard of the CRR. One study (Exp. 106) uses the Track Segment Facility for broad-beam charged particle irradiations of normal human fibroblasts plated on double-sided Mylar dishes to examine genomic instability in irradiated and bystander immortalized small airway epithelial cells (SAEC-htert). These cells were cultured on Mylar dishes and prior to irradiation, half the dish was covered with a metal shield. Cells on the non-covered portion of the dishes were irradiated with 0.1, 1 and 3Gy of ^{4}He ions, while cells on the covered portion of the dishes were bystander cells. Irradiated and bystander populations from each dish were separated and set up in culture. At various times post irradiation (7-28 days) G_2-PCCs were prepared from each culture using Calyculin A. The chromosomes were analyzed by both Giemsa staining (for gross chromosomal aberrations) and mFISH (for more subtle alterations, e.g., translocations). Giemsa staining revealed that both irradiated and bystander populations had elevated yields of chromosomal changes at 7 and 14 days post irradiation.

In a study of the bystander effect in artificial tissue systems (Exp. 130), EPI-200 epithelial tissue samples from MatTek Corp. were irradiated with ^{4}He ions or protons using the Track Segment Facility. Each sample was irradiated with multiple lines of particles down the center. This resulted in a 50μm line of irradiation in the center of a tissue sample 8mm in diameter. Samples were fixed at 15, 30, 45 and 60 minutes post-irradiation and sectioned perpendicular to the line of irradiation. Thus each section of tissue contained both irradiated cells (in the center) and bystander cells (at various distances away from the center). Immunohistochemical protocols were used to examine the expression of various phosphorylated proteins in these sections to determine the role of MAP kinases in the propagation of the bystander response. Enhanced phosphorylation of both Jnk and Erk were seen in both irradiated and bystander cells. Alterations in protein phosphorylation seemed to be dependent on the distance away from the line of irradiation; with closer bystander cells showing higher levels of the phosphorylated proteins.

Hongning Zhou, Yu-Chin Lien and Tom Hei of the CRR continued to use the single-particle Microbeam Facility to try to identify the cell-to-cell signaling transduction pathways involved in radiation-induced bystander mutagenesis (Exp. 110). Using the Microbeam Facility, they found that when 10% of the population of AA8 cells is lethally irradiated, the HGPRT$^-$ mutation frequency was about 4 times higher than the spontaneous yield. However, when 10% of V3 cells in the mixed population (90% AA8 and 10% V3) were irradiated, there was only a limited bystander mutagenesis response in AA8 cells when compared to bystanders of irradiated AA8 cells. A similar result was found when 10% of the AA8 cells in the mixed population (10% AA8 and 90% V3) were irradiated: there was only a limited bystander mutagenesis response in V3 cells when AA8 cells were lethally irradiated. These data indicate that DNA-PKcs deficient cells may have some problems in either delivering or receiving the radiation-induced bystander signals. A fraction of mitochondrial DNA deficient (ρ0) human hamster hybrid (A_L) cells were irradiated in the nucleus or the cytoplasm with ^{4}He ions and given doses that kill essentially all the irradiated cells. Mutagenesis at the CD59 locus for the surviving unirradiated cells was compared with that for wild-type cells. Preliminary data showed that the bystander effect induced by cytoplasmic irradiation was lower in ρ0 cells when compared with similarly irradiated wild-type cells, indicating that mitochondria may partially mediate the process. Interestingly, nuclear irradiation of ρ0 cells induced no bystander CD59 mutation, suggesting that mitochondrial function may play an important role in mediating the bystander signal initiated by nuclear-irradiation. The observed difference of bystander effects between cytoplasmic and nuclear-irradiated ρ0 cells suggests different mechanisms for the genotoxicity and biological consequences of cytoplasmic and nuclear damages. In addition, experiments were performed using the Track Segment Facility. Several cell lines, such as DNA-PKcs deficient cells, mitochondrial function deficient cells and normal human lung fibroblast cells were irradiated on "strip" dishes. They found that 0.5Gy of ^{4}He ions could induce 3.3 times the yield of mutants in AA8 bystander cells compared with the spontaneous background. However, the same radiation increased mutagenesis in bystander cells by a factor of 2.

The occurrence of non-targeted effects calls into question the use of simple linear extrapolations of cancer risk to low doses from data taken at higher doses. Olga Sedelnikova and William Bonner of the NIH, in collaboration with researchers from other institutions, are investigating a model for bystander effects that would be potentially applicable to radiation risk estimation (Exp. 126). They are evaluating the lesions that are introduced into DNA by alpha particles and the resulting non-targeted bystander effect. These lesions, and particularly the most dangerous–the double strand

breaks (DSBs)–can be revealed by the phosphorylation of histone H2AX. Human reconstructed EpiAirway tissues from MatTek Corporation were irradiated with ^{4}He ions in a line 25μm wide across their diameters using the Track Segment Facility and the slit system described above. After irradiation, each tissue was incubated for different time periods, up to 7 days post-irradiation. Control tissues went through the same procedure without being irradiated. A total of 215 tissues were used in the experiment. The tissues were then frozen and shipped to the University of Lethbridge, Canada for extraction of DNA, RNA, histones and proteins, and to the NIH for immunohistochemistry.

Tomoo Funayama, a visitor from the Japan Atomic Energy Agency, explored intracellular mechanisms of the bystander response (Exp. 132). The relationship between cell killing and induction of DNA double strand breaks (DSBs) in the Chinese hamster-human hybrid cell line A_L was analyzed and compared between direct-hit and bystander cells. The cells were irradiated with 0-2Gy of α-particles using the Track Segment Facility and clonogenic survival and induction of γH2AX foci were analyzed. Preliminary results suggest that the intracellular mechanisms of cell killing after induction of DNA double strand breaks are the same for medium-mediated bystander and direct-hit cells. A similar experiment analyzing gap-junction mediated bystander mechanisms using the Microbeam Facility was also carried out. A very limited number of cells in confluent cell colonies were irradiated using a circular irradiation protocol; however, no significant bystander DSB induction was observed.

A group led by Sally Amundson of the CRR continued two types of experiments concerning radiation-induced gene expression profiles in human cell lines using cDNA microarray hybridization and other methods (Exp. 133, 136). One experiment, performed by Shanaz Ghandi and Jaeyong Ahn, involved use of the track segment irradiation for comparison of gene expression responses to direct and bystander irradiation. Normal human fibroblast cells (NHLF and MRC-5) and epithelial cells: AEF-hTERT cells were plated on standard Mylar dishes for direct irradiation or "strip" dishes (see above) for direct-contact bystander irradiations. The cells were irradiated with 125keV/μm ^{4}He ions and assayed for micro-nucleus formation. The main goal of these experiments is to isolate total RNA and protein from the control, irradiated and bystander cells and measure the levels of PTGS-2/COX-2 mRNA and protein. They have found that irradiation with ^{4}He ions induces COX-2 mRNA in the epithelial cells, but the protein is barely detectable. In the case of MRC-5 cells, there are high basal levels of both mRNA and protein but no detectable response to irradiation. After confirmation of the bystander effect in fibroblast cells using the MN assay and/or COX-2 mRNA levels as initial indicators, they are currently using microarray analysis to search for pathways that will suggest novel gene targets involved in the bystander effect. The second experiment, performed in collaboration with Giuseppe Schettino and Surnimal Paul of the CRR, involved irradiation of artificial human tissue samples using the Track Segment Facility. EpiDerm tissues (EPI-200, consisting of fully differentiated cell layers) from MatTek were irradiated in a narrow line (~25μm) with protons having an initial LET of ~10 keV/μm using the same slit masks developed for Sedelnikova's experiment (Exp. 126). After 48h the tissues were removed from the culture insert and cut into narrow slices (200-400mm) parallel to the irradiation line. The strips were fixed on slides and scored for micronucleus formation. Micronucleus induction statistically significantly higher than background level was measured in samples irradiated with as little as 0.1Gy. Although a higher level of micronucleus induction was always detected in the irradiated cells, a bystander response was also measured up to 3mm away with no clear dose dependency.

Peter Grabham and Charles Geard began an assessment of the cytogenetic effects of particles with varying LETs (Exp. 134). Endothelial cells have been subjected to high energy particles at the NASA irradiation facility at Brookhaven National Laboratories and low energy particles at RARAF. Human umbilical vein endothelial cells (HUVECs) were irradiated at RARAF in standard Mylar dishes at varying doses using the Track Segment Facility. Chromosome damage at early stages after irradiation was assessed by giemsa staining. Much like the high energy particles, alpha particles (1Gy) caused widespread gaps and breaks in chromosomes. Studies to examine chromosome aberrations are currently being carried out using FISH analysis.

An investigation to visualize the effects of radiation on chromatin structure in bystander cells using 53BP1 foci as markers of chromatin disorganization in cells was initiated by Keiji Suzuki and Motohiro Yamauchi of Nagasaki University in Japan (Exp. 135). Cells stained with Hoechst 33342 were plated on microbeam dishes along with cells stained with Cell Tracker Red in a ratio of 1:1. Approximately 20% of the cells stained with the Hoechst dye were irradiated with ^{4}He ions using the Microbeam Facility and immunostained. Observation of 53BP1 foci in bystander cells confirmed the indirect effect of radiation on chromatin structure.

Susan Bailey and Eli Williams, a graduate student of Colorado State University, are conducting an experiment to observe recruitment of TRF2 in cells irradiated with α-particles (Exp. 137). Although damage induced by high intensity (e.g., multi-photon) laser irradiation resulted in the positive recruitment of TRF2, α-particles, well known for their ability to produce DSBs, failed to elicit this response. In seeking an explanation for this apparent discrepancy, the possibility was considered that damage from a single α-particle track might be insufficient to cause TRF2 recruitment. To address this issue, they utilized α-particles from the charged-particle Microbeam Facility. Cells were exposed to either 200 or 400 α-particles (roughly equivalent to 30 and 60Gy) in a defined nuclear area of less than 5μm^2 and fixed immediately, 30min, and 60min after irradiation, followed by immunostaining. This resulted in well-defined damage clusters marked by γ-H2AX and MDC1. However, even at these high fluences, producing thousands of DSBs in a limited nuclear volume, TRF2 recruitment was not observed.

Edouard Azzam, Janine Santos and Olga Kovalenko of the New Jersey School of Medicine and Dentistry are investigating whether mitochondrial DNA (mtDNA) damage by

itself can trigger apoptosis in hTERT cells (Exp. 138). Parental cells carrying wild type or a nuclear-only hTERT mutant are irradiated either in the nucleus or the cytoplasm using the Microbeam Facility, allowed to recover for approximately 24h, and stained with YOPRO-1 in order to score the percentage of apoptotic cells. Using the above cells and apoptosis as an endpoint, they are also investigating the expression of radiation-induced bystander effects under conditions wherein a small fraction of cells in the exposed population is targeted through the nucleus or cytoplasm by one or more ^{4}He ions.

Development of facilities

This year our development efforts concentrated on a number of extensions of the capabilities of our microbeam facilities including:

- Development of focused accelerator microbeams
- Non-scattering particle detector
- Advanced imaging systems
- Focused x-ray microbeam
- New laboratory space

Development of focused accelerator microbeams

The first quadrupole triplet for the double quadrupole lens, installed in 2003, continues to operate very reliably, with very few sparks. It has proven to be quite robust, surviving vacuum excursions caused by the occasional breakage of the ion beam exit window. An electrostatic phase space "confuser" has been installed just above the 90° bending magnet. By varying the voltages on 4 electrodes, the beam is continually steered in a non-repetitive way to eliminate any correspondence between particle position and direction. This has enabled us to focus a 6MeV ^{4}He beam down to a diameter of 2μm.

The parts for the second quadrupole triplet have been constructed in our shop and will be inserted into a separate alignment tube for testing, in place of the present lens once the permanent magnet microbeam (Fig. 1) is fully operational for biological irradiations. When the voltages on this second lens have been adjusted to produce the smallest beam spot attainable, the two lenses will be mounted in a single tube for testing of the compound lens system that will produce a sub-micron beam spot. After using this sub-micron beam for biological irradiations for a suitable period, the testing process will be repeated with two more triplet lenses so that we will eventually have two complete compound lenses, one of which will be used as a spare.

A second microbeam has been reassembled after construction of the 3rd floor. A beam of 5.3MeV ^{4}He ions or protons will be focused into a spot smaller than 10μm in diameter using a compound quadrupole triplet lens made from commercially available permanent magnets. Because the magnet strengths are essentially fixed, only a single energy proton or ^{4}He ion can be focused. The pair of quadrupole triplets is similar to the one designed for the sub-micron microbeam, the only difference being that it uses magnetic rather than electrostatic lenses. This system was originally designed to focus alpha particles from a ^{210}Po source during the dismantling of the Van de Graaff and the installation of

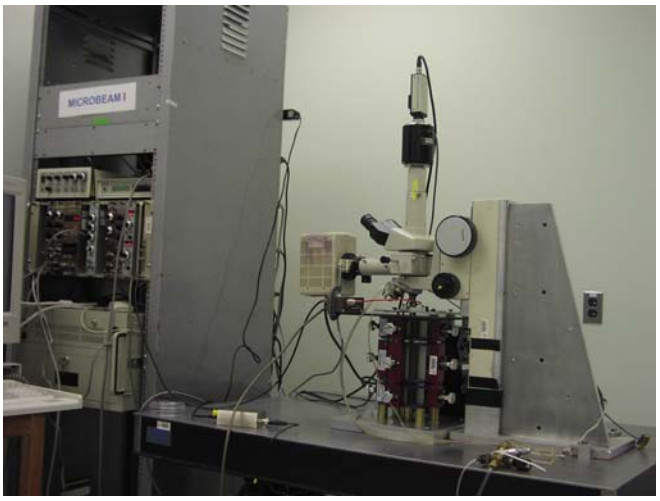

Fig. 1. A view of the Permanent Magnet Microbeam system in its new lab on the 3rd floor.

the Singletron. Using a charged particle beam from the accelerator will provide us with a much greater flux. The endstation for our original microbeam has been moved from the 2nd floor, where it was used for the collimated microbeam, to the new microbeam lab on the 3rd floor because additional room for the lens structure is required between the focal point and the final bending magnet

The helium beam from the Singletron accelerator is incident on a thin aluminum foil to produce a beam in which the particle location and direction are not coupled. This foil will soon be replaced by a magnetic steerer, which will reduce the energy spread in the beam, allowing the beam to be focused to a smaller diameter, and increasing the flux at the endstation. The lenses have been optically aligned and adjustment of the quadrupole magnet strengths has begun using micrometric screws to retract and extend the individual magnets of each quadrupole.

This system will be used for irradiations when the electrostatic system is unavailable because of development or repair.

Non-scattering particle detector

To irradiate thick samples, such as model tissue systems or oocytes, to use particles with very short ranges, such as the heavy ions from the laser ion source, and to allow irradiation of cell monolayers without removing the culture medium, a completely non-scattering particle detector is necessary upstream of the samples. A novel particle detector has been designed on the basis of a long series of inductive cells coupled together into a delay line. The Lumped Delay Line Detector (LD^2) will consist of 300 silver cylinders 3mm long with a 2.2mm inside diameter connected by inductors and capacitively coupled to ground. The cylinders are glued to a semi-cylindrical tube of dielectric material 1m long for mechanical support. The dielectric has a semi-cylindrical metal tube around it that can be rotated about its axis to adjust the capacitance. If the individual segment delays are set (by adjustment of the capacitance) such that the propagation velocity of the pulse equals the projectile velocity, the pulses capacitively induced in all segments by the passage of a single

charged particle will add coherently resulting in a fast electron pulse at each end of the delay line that is 150 times larger than the charge induced on a single cylinder. This easily detectable charge of at least 150 electrons will be amplified to provide the detection pulse for the particle counter. Two prototype LD^2 detectors (1/6 length) have been constructed for testing their signal propagation properties. Based on these results the parameters for a full-length LD^2 detector have been determined. The full-length detector is currently under construction. It is anticipated that this detector will become the standard detector for all microbeam irradiations.

Advanced imaging systems

Development continued on new imaging techniques to view cells without using stain and to obtain three-dimensional images of unstained cells. Two different techniques continue to be investigated: quantitative non-interference phase microscopy (QPm) and immersion-based Mirau interferometry (IMI). Both have been integrated into the Microbeam Facility and are being tested for applicability to rapid location and targeting of cells for microbeam irradiation without use of stain.

QPm is a non-interferometric approach to non-stain imaging. Reflected light images are obtained in focus and with the focus set slightly above and below the sample plane. These images are then used to approximately solve the light transport equation using the Fourier transform-based software from Iatia Vision Sciences. The results are used to create a new 2D map of the sample which is then fed back into the custom microbeam irradiation software. By streamlining the control program, including interleaving the image processing steps with the mechanical motions of the stage, the additional processing time required to convert the raw images into QPm images can be reduced such that it affects throughput by only about 10%. We are working with Iatia to improve this processing time by taking full advantage of the on-board dual processing, which will cut this factor in half.

In tests, some cells have been missed and there also have been false positives. In general, the quality of the images can be improved by carefully optimizing tuning of the parameters for the approximate solution to the transport equation. However, to optimize for our regular, automated use there is still work to be done in eliminating false cells and reducing missed cells. Several variables have been isolated and eliminated as causes: plating time, cell-type, cell phase, light color, cell growth surface, amount of medium (depth), percent of medium vs. buffer, and use of a cover glass. Continued efforts are aimed at finding a combination of these variables that may affect the images and at exploring other variables that have not yet been considered.

The immersion-based Mirau interferometric (IMI) objective is currently under construction (Fig. 2) and has been designed to function as an immersion lens with standard interferometric techniques using a short coherence length and to otherwise accommodate the endstation requirements for the microbeam at RARAF. The preliminary results in air on 10μm polystyroid beads were sufficiently encouraging to warrant the effort to design the new objective. As part of the testing for the design process we modified an off-the-shelf Mirau objective such that it became a water immersion lens, and we confirmed that the two equal-arm light pathways will indeed be restored and will then provide interference fringes in the environment with sufficient contrast to perform the biological experiments.

Preliminary results from the modified objective confirm that the contrast will be sufficient. The finished objective will support rapidly and automatically locating the cell nuclei under the no-stain scenario. “Banding” in some of the images indicates that further work must be done to eliminate both a slow drift in z-position and some very slight vibrational interference.

While it is possible that we ultimately will keep both forms of no-stain imaging in the endstation, QPm and IMI are being evaluated in competition with each other. Under consideration are: processing time, reliability, maintenance, and ease of use for the experimenter. IMI is slightly faster in the endstation under regular use than QPm but both are acceptable. QPm is likely to be improved, so they will score about the same. IMI, judging by the preliminary images, is much more reliable than QPm at this stage. QPm is a software solution and does not require introduction of fluids or cleaning, whereas IMI does. QPm does not require any additional equipment and can work in air, while the immersion-Mirau interferometer requires the end-user to use a custom objective and an immersion-based approach. It appears likely that the immersion-Mirau approach will ultimately be favored, but additional work will be done especially on the QPm reliability.

We are constructing a multi-photon microscope for our single-cell single-particle Microbeam Facility to detect and observe the short-term molecular kinetics of radiation response in living cells and to permit imaging in thick targets, such as tissue samples. The multi-photon capability is being built into the Nikon Eclipse E600-FN research fluorescence microscope of the microbeam irradiation system and will provide three-dimensional imaging. A Chameleon (Coherent Inc.) tunable titanium sapphire laser (140fs pulses at a 90MHz repetition rate) is the source for the multi-photon excitation. The scan head incorporates commercial scanners and a scan lens then focuses the laser beam to a point at an

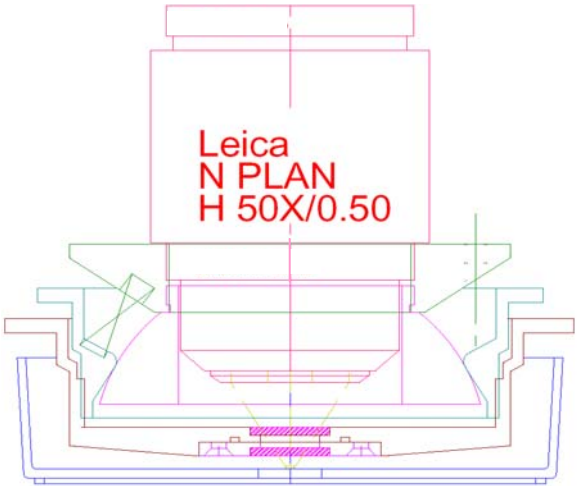

Fig. 2. Construction drawing of the immersion Mirau lens.

image plane of the microscope (a CCD camera is also placed at such an image plane for fluorescent microscopy). The incident laser beam will enter the microscope through the side of the trinocular tube of the microscope. A switch mirror will allow us to choose between multi-photon microscopy and standard fluorescence microscopy. The scanned laser beam establishes an optical section within the specimen, where multi-photon absorption preferentially occurs. Wavelengths available from the laser can penetrate to depths of about 100 microns in a biological sample by varying the z-position of the specimen stage. Returning along the collection pathway, light emitted from the specimen is selectively deflected by a series of dichroic mirrors to an array of photomultiplier tubes (PMTs). To control the multi-photon microscope, we are adopting the design and software of Karel Svoboda, Cold Spring Harbor.

Focused x-ray microbeam

There are considerable benefits in using soft x-ray microbeams for both mechanistic and risk estimation endpoints. The higher spatial resolution achievable with modern state-of-the-art x-ray optics elements combined with the localized damage produced by the absorption of low-energy photons (~1-5keV) represents a unique tool to investigate the radio-sensitivity of sub-cellular and eventually sub-nuclear targets. Moreover, as these x-rays do not suffer from scattering, by using higher energy x-rays (~5keV) it is possible to irradiate with sub-micron precision individual cells and/or part of them up to a few hundred microns deep inside a tissue sample in order to investigate the relevance of effects such as the bystander effect in 3D structured cell systems.

We have investigated expanding the microbeam to include soft x-rays, characteristic K_α x-rays from Al (1.49keV) and Ti (4.5keV). The use of higher energies is not feasible due to Compton scattering effects; we are limited to x-ray energies where the predominant mode of interaction is photoelectron absorption.

Zone Plate (ZP) lenses will de-magnify to a micron or sub-micron size spot a small X-ray source (i.e.~100μm D) produced by bombarding a thin solid target with high-energy protons using a microbeam triplet lens. We investigated the production of characteristic x-rays (K_α line) as a function of the proton energy for aluminum and titanium. The best x-ray production cross sections are at 2.9MeV for Al and 4.5MeV for Ti. By using the already focused proton microbeam to generate characteristic x-rays, it is possible to obtain a nearly monochromatic x-ray beam (very low bremsstrahlung yield) and a reasonably small x-ray source (~10μm diameter), reducing requirements on the subsequent x-ray focusing system.

The present design consists of 3 thin Al or Ti foils 15-20 μm thick separated by 5μm gaps through which cooled He is blown. Such a target is able to cope with a substantial amount of power from the proton beam, providing an x-ray dose rate suitable for many radiobiological experiments (~0.05Gy/sec), even with a sub-micron diameter photon beam. This target design has been tested with a laser beam by focusing 0.8W (800nm) into a 99μm spot. The measurements have exceeded the expectations based on simulations performed using a finite element analysis program (ANSYS), indicating that the designed target is able to cope with a considerable amount of power from the proton beam.

Based on these data, zone plate specifications have been worked out. The proposed zone plate will have a radius of only 80μm and an outmost zone width of 40nm, which implies a zone plate which is easy to manufacture (focusing efficiency closer to the maximum theoretical value) and easy to handle. The new zone plate will be placed close to the x-ray source (150mm) and have a focal length of 12.57mm (demagnification factor of ~12). The final expected dose rates to the sample, based on ANSYS simulations, are 0.03 to 0.6Gy/s for beam spots 0.4 to 2.1μm in diameter.

The main elements of the system have been manufactured in our machine shop and the zone plates are scheduled to be purchased this year.

New laboratory space

Because of a large homeland security research and development grant received by David Brenner and Gerhard Randers-Pehrson from the National Institute of Allergy and Infectious Diseases (NIAID), the Trustees of Columbia University contributed the funds required to build over 2000 square feet of new laboratory and office space on the third floor of the facility (Fig. 3). When RARAF was built in the early 1980s, this space had been intended for offices and a meeting room. Since there were never funds available to build these, the space had been used for storage. Construction began in April 2006 and was completed in December. Over half the area is a biology laboratory with provision for

Fig. 3. Layout of the third floor of RARAF. Microbeam Lab III (permanent magnet lens system) is directly above the original microbeam laboratory. The wall on the left is ~58 feet long. Microbeam II, which houses the electrostatic lens system, is shown in the bottom right of center and is a half-floor below the new construction, shown with emphasized walls.

Fig. 4. The new Biology Lab as viewed from the entrance to the third floor lab space (upper right in Fig. 3). In view are the two islands that have work stations for up to 12 people. Sasha Lyulko is working in the new lab.

three laminar flow hoods, one of which is a class II hood, several incubators, refrigerators and freezers and two islands comprising a dozen work stations (Fig. 4). There are also six desks for technicians and postdocs. Two of the labs are a dedicated microscopy laboratory (Fig. 5) with three workstations and a physics laboratory that is being used for the NIAID project.

Included in the construction is a new lab for the permanent magnet Microbeam Facility. While this system was being developed as a stand-alone microbeam for use with a ^{210}Po alpha source, it was housed in a makeshift room on the 3rd floor. The magnetic quadrupole quadruplets and endstation for the system were removed before construction began. Now that construction is complete, the beam line has been reconstructed with the two quadruplet lenses, and the endstation with the microscope and electronics has been installed. The lab is fitted with a laminar flow hood and an incubator. The magnet system is being adjusted to provide the best focusing using proton and helium ion beams from the accelerator. When the focusing studies are complete, the system will be available again for biological irradiations.

Fig. 5. Dr. Brian Ponnaiya, Associate Research Scientist, is working in the new microscope laboratory on the third floor.

Singletron utilization and operation

Accelerator usage is summarized in Table 2. The Singletron was started at 7:30 AM on most days, often run into the evening, and occasionally run on weekends for experiments, development and repair. This has resulted in a total use that equals the nominal accelerator availability of one 8-hour shift per weekday.

Use of the accelerator for radiobiology and associated dosimetry increased by more than 10% over 2004-2005 to the highest level since RARAF has been at Nevis Labs and was about 30% higher than the average for 2000 to 2005. Over half the accelerator use for all experiments was for microbeam irradiations and 23% for track segment irradiations.

The Microbeam Facility is in great demand because it enables selective irradiation of individual cell nuclei or cytoplasm. In addition, because of the relatively low number of cells that can be irradiated in a day, microbeam experiments usually require considerably more beam time than broad beam (track segment) irradiations to obtain sufficient biological material, especially for low probability events such as mutation and bystander effects.

The Track Segment Facility is being used more efficiently, reducing the amount of accelerator time required to satisfy user demand. Because the irradiation times for samples are often 10 seconds or less, multiple users, sometimes as many as 5, are run on a single shift, sometimes using different LETs and different types of ions in the same day.

Radiological physics utilization of the accelerator increased slightly this past year, consisting mainly of the experiment to develop a system to detect explosives in luggage (Exp. 82).

Approximately 20% of the experiment time was used for experiments proposed by outside users, about 2/3 the average for the last five years. This is probably to be expected since operations had been interrupted for the last 6 months of 2005 due to the replacement of the Van de Graaff and it takes a while to get back up to speed.

Use of the accelerator for online development decreased by about 50% from last year. This is predominantly due to the fact that in 2005 there was a major push to get the stand alone microbeam system operational and this past year the emphasis was on radiobiology, to catch up for the 6 months required for the replacement of the accelerator .

Accelerator maintenance and repair time declined somewhat relative to last year, returning to the levels of 1986-2001 when the previous accelerator was running well. The new Singletron accelerator has operated reliably for over 15 months with a single exception: the RF power supply for the ion source. The accelerator has maintained a terminal potential as high as 5.5MV without sparking and probably can maintain an even higher voltage. No accelerator maintenance or repairs have been required for the charging and control systems. The RF tubes for the ionization source were replaced several times, each requiring an accelerator opening, before it was determined that the voltage from the terminal generator was too high. The system was assembled and tested in the Netherlands, where the electric system operates at 50 cycles per second. In the United States, the

Table 2. Accelerator Use, January–December 2006
Percent Usage of Available Days

Radiobiology and associated dosimetry	47%
Radiological physics and chemistry	12%
On-line facility development and testing	26%
Safety system	2%
Accelerator-related repairs/maintenance	8%
Other repairs and maintenance	3%
Off-line facility development	15%

system operates at 60cps. The higher frequency caused the motor that drives the generator to operate at a higher speed, which produced a higher supply voltage. A transformer tap for the RF supply was moved to a different position, lowering the voltage. The RF source has worked reliably for the last 9 months. There was one accelerator opening to replace the ion source bottle, which had become dirty after a year of service.

The terminal voltage, as expected, has very low ripple and produces beams with very little energy spread. Measurements of the Li(p,n) threshold show a very sharp rise in yield with terminal voltage because of the narrow beam energy. An unexpected feature of the accelerator has been some drift in the terminal voltage as the accelerator warms up after starting. The beam currents used for the microbeam irradiations are not large enough to permit slit regulation; therefore the GVM is the main control of the terminal voltage. Because the beam energy is so narrow, beam intensity decreases rapidly as the terminal potential changes by a few kilovolts during warm-up. The problem has been traced to changes in the spacing of the pick-up plates in the generating voltmeter (GVM) as the accelerator warms up. The GVM housing is presently being heated to a constant temperature at all times, greatly reducing the voltage change during warm-up. A more complex system is being constructed that will adjust the temperature of the GVM housing based on the load on the motor that rotates the GVM blades.

Training

The Small Group Apprenticeship Program continued for the third year. Five students from Stuyvesant High School in Manhattan spent at least two half-days each week for six weeks during the summer working on projects in biology or physics (Fig. 6). Stuyvesant is a high school specializing in science that is open to students throughout New York City by competitive admission. The students gave professional PowerPoint presentations to our group at the end of the program. Below is a list of the titles of the work presented followed by the name of the student and the name of his or her mentor:

1. The Bystander Effect: MAP Kinases and their roles in the phenomenon; JNK and Apoptosis – Kelvin Wong (Brian Ponnaiya).
2. Multiphoton Microscopy Prototype Design – Anthony Pang (Alan Bigelow).

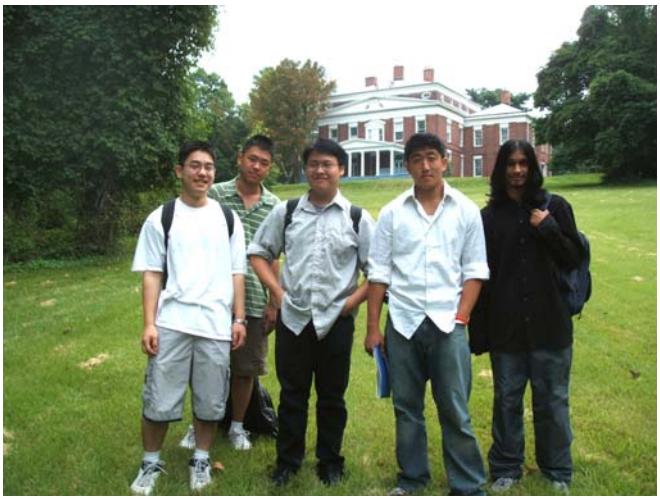

Fig. 6. Stuyvesant High School students who participated in the 2006 Small Group Apprenticeship Program (l-r): Edward Sung, Raymond Wu, Anthony Pang, Kelvin Wong and Ridwan Sami.

3. The Biological Effect of Dirty Bombs – Raymond Wu (Giuseppe Schettino).
4. Beam Stuff; Calculator Program – Ridwan Sami (Gerhard Randers-Pehrson).
5. Progress on the LD^2 Detector: Summer of '06 – Edward Sung (Guy Garty).

Several of the previous students have been co-authors of scientific journal articles, including one that was published in the prestigious Proceedings of the National Academy of Science (PNAS).

Dr. Tomoo Funayama of the Japan Atomic Energy Agency, who arrived in November, 2005 for a one-year visit at RARAF, returned to Japan in November, 2006. Dr. Funayama worked with Charles Geard and learned to perform experiments using the Microbeam and Track Segment Facilities.

Andrei Popescu, a student at Ossining High School in Westchester County, NY, is working with Brian Ponnaiya over the next year. He will be studying DNA breakage and micronucleus formation in mouse cells after x-ray irradiation.

Dissemination

A highlight this year was our hosting the 7th International Workshop of Microbeam Probes of Cellular Radiation Response, held at the Morningside campus of Columbia University, March 15-17, 2006. The two-day workshop featured over 100 scientists from eleven different countries.

RARAF also hosted an open house the day prior to the start of the Workshop. More than 35 researchers from around the world toured RARAF and received briefings on the new accelerator, the irradiation facilities and the research being conducted. Visitors also had opportunities to ask questions and have short discussions with the staff.

In October there was a tour of RARAF by 23 students and three professors from Concordia College in New Rochelle, NY.

Personnel

The Director of RARAF is Dr. David Brenner. The accelerator facility is operated by Mr. Stephen Marino and Dr. Gerhard Randers-Pehrson.

Dr. Alan Bigelow, an Associate Research Scientist, is continuing the development of the laser ion source and has begun the development of a two-photon microscopy system using a fast laser.

Dr. Guy Garty, a Staff Associate, is developing the secondary emission ion microscope (SEIM) and an inductive detector (LD^2) for single ions.

Mr. Greg Ross, a Programmer/Analyst, left RARAF in May. He had been assisting with various programming tasks and worked on new methods of imaging cells without stain.

Dr. Giuseppe Schettino, a Postdoctoral Fellow who left RARAF in December, worked primarily on the development of the x-ray microbeam and performed some biological experiments using tissues grown in culture.

Sasha Lyulko, a graduate student in the Physics Department at Columbia, began working at RARAF in September. She is learning to perform microbeam irradiations, will be involved in research in methods to image cells without stain, and spends half her time working for the NIAID project.

Two new postdocs arrived on the same day in January, 2007: Dr. Andrew Harken, who recently received his Ph.D. in Chemicals Material Engineering from the University of Nebraska at Lincoln, and Dr. Yanping Xu, who recently received his Ph.D. in Physics from North Carolina State University.

Several biologists from the Center for Radiological Research are stationed at the facility in order to perform experiments:

- Dr. Charles Geard, the Associate Director of the CRR and the Senior Biologist for the P41 grant that is the major support for RARAF, continues to spend most of each working day at RARAF. In addition to his own research, he collaborates with some of the outside users on experiments using the single-particle Microbeam Facility.
- Dr. Brian Ponnaiya is an Associate Research Scientist performing experiments using the Track Segment and Microbeam irradiation facilities.
- Ms. Gloria Jenkins, a biology technician, performs experiments on the Microbeam Facility for Dr. Geard. Unfortunately, Gloria will be retiring in May of 2007.
- Dr. Alexandre Mezentsev, an Associate Research Scientist, is working with cultured tissue systems and is starting to spend almost half his time at RARAF.

At the end of March, Yigal and Atara Horowitz from Ben Gurion University in Israel began a 1-year sabbatical at RARAF. Their project will be "Charged Particle Characterization of 'Slow-Cooled' LiF:Mg,Ti (TLD-100)" using the Track Segment broad beam irradiation facility.

Recent publications of work performed at RARAF (2005-2006)

1. Brenner DJ. Editor, The 7th International Workshop on Microbeam Probes of Cellular Radiation Response. *Radiat* Res **166**:652-89, 2006.
2. Calaf GM, Roy D and Hei TK. Growth factor biomarkers associated with estrogen- and radiation-induced breast cancer progression. *Int J Oncol* **28**:87-93, 2006.
3. Garty G, Ross GJ, Bigelow AW, Randers-Pehrson G and Brenner DJ. Testing the Stand-Alone Microbeam at Columbia University. *Radiat Prot Dosimetry*, 2006.
4. Hei TK. Cyclooxygenase-2 as a signaling molecule in radiation induced bystander effect. *Mol Carcinogenesis* **45**:455-60, 2006.
5. Ivanov VN, Zhou H and Hei TK. Gamma-irradiation and alpha-particle exposure sensitize human melanoma cells to TRAIL-mediated apoptosis through upregulation of TRAIL-R2/DR5 expression and translocation to the cell surface. *Exp Cell Res.* (submitted 2007)
6. Maurer RH, Zeitlin CJ, Haggerty DK, Roth DR and Goldsten JO. Compact Ion and Neutron Spectrometer (CINS) for Space Application. 2005 IEEE Nuclear Science Symposium Conference Record, N14-48, pp 428-432, Puerto Rico, 23-29 October 2005.
7. Ponnaiya B, Jenkins-Baker G, Randers-Pherson G and Geard CR. Quantifying a bystander response following microbeam irradiation using single cell rt-pcr analyses. *Exp Hematology* (accepted 2007).
8. Roy D, Calaf GM, Hande MP and Hei TK. Allelic imbalance at 11q23-q24 chromosome associated with estrogen and radiation-induced breast cancer progression. *Int. J. Oncol.* **28**:667-74, 2006.
9. Sedelnikova OA, Nakamura A, Kovalchuk O, Koturbash I, Mitchell SA, Marino SA, Brenner DJ and Bonner WM. DNA double-strand breaks form in bystander cells after microbeam irradiation of three-dimensional human tissue models. *Cancer Res* (accepted 2007).
10. Sykora GJ, Akselrod MS, Salasky M and Marino SA. Novel fluorescent nuclear track detectors for passive neutron dosimetry. *Radiat Prot Dosimetry* pp.1-6, 2007. doi:10.1093/rpd/ncm058.
11. Williams ES, Stap J, Essers J, Ponnaiya B, Luijsterburg MS, Krawczyk, PM, Ullrich, RL, Aten JA and Bailey SM. DNA double strand breaks are not sufficient to initiate the recruitment of TRF2. *Nature Genetics* (accepted 2007). ■